JOURNAL OF THERMOPHYSICS AND HEAT TRANSFER
Vol. 9, No. 1, January–March 1995

Depriming/Rewetting of Arterial Heat Pipes: Comparison with Share-II Flight Experiment

J. M. Ochterbeck* and G. P. Peterson†
Texas A&M University, College Station, Texas 77843
and
E. K. Ungar‡
NASA Johnson Space Center, Houston, Texas 77058

Utilizing several previously developed analytical expressions, a combined analytical and numerical model was developed to analyze the deprime and reprime/rewetting characteristics of two high-capacity external artery heat pipe designs undergoing externally induced accelerations. The analysis considered three distinct phases of the deprime and reprime/rewetting process: 1) the effect of longitudinal accelerations on the depriming, 2) the time required for repriming of the liquid artery once the longitudinal acceleration had been terminated, and 3) the rewetting characteristics of the circumferential wall grooves. Combining these three processes, a technique was developed by which the effect of external accelerations on the operational characteristics of the external artery heat pipes could be predicted. The results of this analysis were then compared with the experimental results obtained from acceleration tests on these two heat pipe configurations conducted aboard STS-43 in August 1991. The depriming analysis indicated the importance of frictional effects on the liquid configuration during an external acceleration. In addition, the evaporator recovery time of the heat pipe was found to be dominated by the liquid artery reprime/rewetting characteristics as opposed to the characteristics of the circumferential wall grooves. Overall, this technique compared favorably with the microgravity flight results and confirmed the accuracy of the analytical techniques.

Nomenclature

A = channel area
a = acceleration
c_p = specific heat
c_1 = constant defined in Eq. (5)
F = force
H = length of liquid column
h_f = latent heat of vaporization
L = length of heat pipe
m = mass of liquid column
$\dot{m}$ = mass flow rate
P = perimeter
Q = heat input
R = radius
r = circumferential groove radius
t = time
U = liquid column velocity
U_w = rewetting velocity
v_s = velocity through the slot
ΔT = level of wall superheat
δ = width of the slot
μ = absolute viscosity
ρ = density
σ = surface tension
τ = time
τ_w = wall shear stress

Subscripts
c = cross-sectional or condenser
e = evaporator
eff = effective
g = groove
l = liquid
s = solid or heat pipe case material
t = transport
v = vapor

Presented as Paper 93-0282 at the AIAA 31st Aerospace Sciences Meeting, Reno, NV, Jan. 11–14, 1993; received Oct. 15, 1993; revision received March 18, 1994; accepted for publication July 20, 1994.

*Currently Assistant Professor, Department of Mechanical Engineering, Clemson University, Clemson, SC 29631. Member AIAA.
†Tenneco Professor of Mechanical Engineering, Department of Mechanical Engineering. Associate Fellow AIAA.
‡Senior Thermal Analyst, Crew and Thermal Systems Division. Member AIAA.

Introduction

THE Space Station Freedom (SSF) External Active Thermal Control System (EATCS) is designed to transport waste heat from widely distributed heat acquisition sites in the crew modules and power conversion devices to the radiator system, where it is radiated to space.[1] This system consists of three two-phase ammonia heat transport loops, which pump liquid ammonia to the heat acquisition sites where it is partially evaporated and returned to the pump module. The liquid and vapor are then separated and the vapor is pumped to the radiator system, where it is condensed and subcooled. The design requirements of SSF (75-kW electrical power, a projected radiator area of 390 m^2, and a planned lifetime of 30 yr) have led to the consideration of several radiator systems. Because heat pipe radiators are modular in nature and thereby relatively insensitive to punctures by micrometeoroids and orbital debris, these have received considerable attention. One heat pipe radiator option requires transport lengths of 6.7 m and a transport capacity of 425 W for each individual heat pipe. These requirements led to the consideration of two external artery heat pipe designs, the monogroove[2] heat pipe and the graded groove[3] heat pipe. Both of these designs were flown onboard the Space Shuttle (STS-43 in August 1991) as part of the Space Station Heat Pipe Advanced Radiator Elements (SHARE II) heat pipe experiment, and utilize separate liquid and vapor channels connected by a longitudinal, or axial, slot that provides axial pumping.

Previous analytical[4] and experimental[5] investigations have demonstrated that these heat pipes will passively prime in 0 g environments, however, orbital attitude adjustments, reboost, and docking maneuvers may all result in accelerations sufficient to cause redistribution of the liquid within the heat pipes. For the situation of accelerations along the longitudinal heat pipe axis, two cases can occur: 1) the evaporator will be flooded by liquid or 2) the evaporator will dry out. If simultaneous dryout occurs in multiple heat pipes, the heat rejection capability of the radiator system may be severely impaired.

Recently, the effects of acceleration-induced depriming have been investigated analytically.[6] This investigation specifically addressed the acceleration effects for external artery or longitudinally grooved heat pipes, similar to those considered for SSF. When the magnitude and/or duration of the acceleration is sufficient, liquid will flow out of the liquid channel through the connecting slot and accumulate in the ends of the liquid and vapor channels opposite the direction of acceleration. For accelerations in the direction of the evaporator, dryout may easily occur.

To predict the performance of the radiator system following a dryout, the process of repriming the heat pipe evaporator must be evaluated. In the case of external artery heat pipes connected to a two-phase EATCS, two complicating factors exist. First, the EATCS interface will be flooded with vapor at the bus set-point temperature following heat pipe dryout. Thus, the heat pipe must rewet against a constant temperature boundary condition, which can result in extremely high local heat fluxes. Second, both the monogroove and graded groove heat pipes contain circumferential grooves in the vapor channel to increase the local heat transfer coefficient by providing a uniformly distributed thin film region from which vaporization can occur. For this reason, the rewetting of the wall grooves in the evaporator must be modeled in addition to the rewetting of the evaporator liquid artery.

Once dryout of the evaporator has occurred, the primary concern is then how the heat pipe channels will reprime and the wall grooves rewet. An analytical and experimental investigation of the rewetting characteristics of grooved circular channels has been conducted.[7] A theoretical description of the mechanisms that govern the rewetting front were developed and compared with SHARE II experimental results for grooved surfaces with variations in the applied heat flux.

SHARE II Test Articles

The SHARE II experiment flew on STS-43 in August 1991 and tested two 6.7-m-long, high-capacity heat pipes, one monogroove and one graded groove. Each heat pipe was encased in a 0.15-m fin and was fastened to a box support beam mounted on the starboard sill of the Space Shuttle payload bay. Electric heaters were used for heat input, and heat was rejected to the space environment through one side of the fins.

The monogroove heat pipe[2] was designed jointly by NASA Johnson Space Center and the Grumman Aerospace Corporation (GAC), and was a redesign of the original Space Station Heat Pipe Advanced Radiator Element (SHARE) heat pipe flown on STS-29 in March 1989.[8] Because of problems with an internal hydraulic mismatch and a non-self-priming manifold design in the SHARE experiment, the flight test was less than fully successful. The NASA/GAC heat pipe was designed to address the shortcomings of the SHARE experiment and to be less sensitive to noncondensible gas (NCG) supported vapor bubbles in the liquid artery.[2] As shown in Fig. 1a, the monogroove heat pipe extrusion consists of a 14.9-mm-diam vapor channel that is connected to a 10.2-mm-diam liquid artery by a 0.25-mm-monogroove slot. The heat pipe evaporator, transition, and condenser lengths were 0.61, 0.61, and 5.46 m, respectively, and the vapor channel in the evaporator and condenser was threaded with circumferential wall grooves. The evaporator and transition sections of the liquid artery contained a screen wick insert to provide alternate feed paths to the wall grooves in the event that a NCG-supported vapor bubble was ingested into the liquid artery wick. To reduce the size of any vapor bubbles in the evaporator screen wick, the liquid and vapor channels were separated in the transition zone to allow subcooling of the liquid prior to entering the evaporator. In this way, the heat pipe could continue to operate normally, even if NCG supported vapor bubbles were present in the evaporator liquid channel.

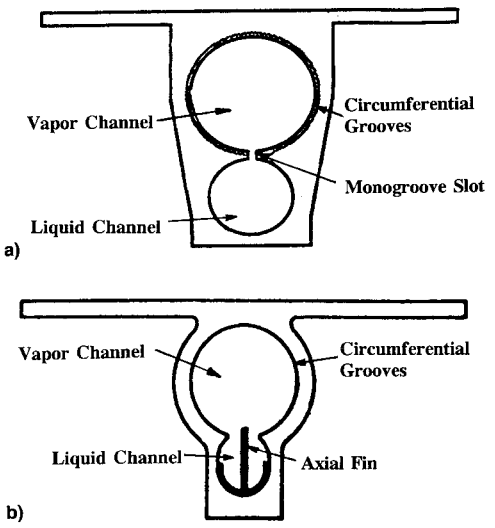

Fig. 1 a) Monogroove[2] and b) graded groove heat pipe extrusions.

The graded groove heat pipe[3] was designed by Lockheed Missiles and Space Corp. and LTV Missiles and Space Corp. (LMSC/LTV), and also was designed to prevent problems encountered in the SHARE heat pipe design[8] and to address potential NCG problems. The graded groove heat pipe extrusion, shown in Fig. 1b, utilized a 14.6-mm-diam vapor channel connected to a 7.9-mm nominal diam liquid artery by a 3.8-mm slot. The evaporator and condenser lengths were 0.76 and 5.94 m, respectively. The heat pipe vapor channel was threaded with circumferential grooves, and the liquid channel cross section was designed such that NCG supported vapor bubbles large enough to completely fill the channel would vent easily through the slot, thus avoiding interruption of the liquid flow. The hydraulic diameter of the liquid artery was graded by the insertion of a 1.02-m-long liquid channel splitter in the evaporator end. This splitter reduced the slot width and liquid channel hydraulic diameter, thus increasing the capillary pumping in the evaporator section without greatly increasing the overall resistance to liquid flow.

SHARE II Flight Tests

In addition to the numerous microgravity heat pipe performance tests carried out on the SHARE II experiment,[9,10] three depriming/repriming tests were performed using an imposed Space Shuttle acceleration. In each test, the Primary Reaction Control System (PRCS) thrusters were fired to provide an acceleration of 0.076 ± 0.015 m/s^2 along the longitudinal heat pipe axis. In each case the acceleration was in the direction that would force liquid from the evaporator end to the condenser end of the heat pipe. Immediately after the acceleration, the Space Shuttle attitude was stabilized and the vehicle was placed in free drift to minimize disturbances to the heat pipes. The operating conditions and general results for each heat pipe and corresponding tests are summarized in Table 1. In Deprime test no. II, the heat load was increased stepwise from zero to full load 4 min prior to the PRCS jet firing, whereas in Deprime test no. III, the heat load was initiated 1 h prior to the jet firing.

Analysis

The current investigation separates the deprime/reprime analysis into two distinctive sections. First, the liquid distri-

Table 1 Summary of SHARE II Deprime tests

Test no.	MET, h	PRCS duration, s	NASA/GAC—monogroove Power, W	NASA/GAC—monogroove T_{cond}, °C	NASA/GAC—monogroove Deprime	LMSC/LTV—graded groove Power, W	LMSC/LTV—graded groove T_{cond}, °C	LMSC/LTV—graded groove Deprime
I	115.1	1	127	20	No	127	20	No
II	117.2	8	418	0	Yes	427	−6	Yes
III	168.8	5	237	27	No	240	27	Yes

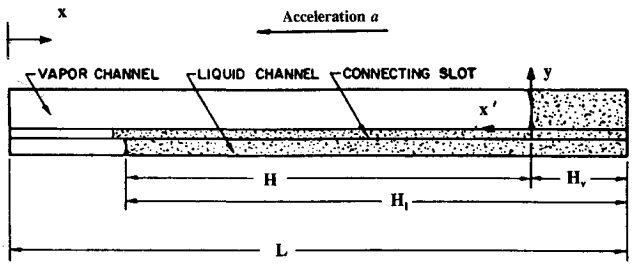

Fig. 2 Location of the liquid level in the liquid and vapor channels.

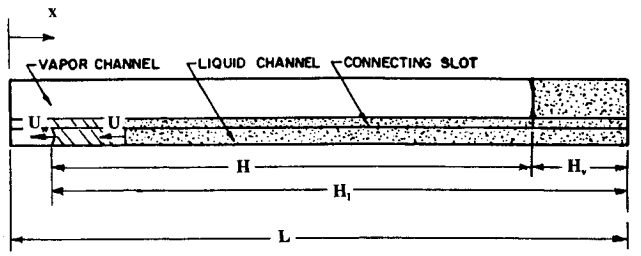

Fig. 3 Physical model for the arterial repriming/rewetting location and velocity.

bution during the deprime (acceleration) tests are evaluated. This is then followed by the analysis of the reprime/rewetting characteristics of the liquid channel and circumferential wall grooves. The geometry of the basic arterial heat pipe configurations allows the reprime/rewetting characteristics to be determined by superposition. The superposition technique assumes that the axial flow and the circumferential wall groove flow are essentially independent, because wall priming at any location cannot occur until the axial slot is filled with liquid. This procedure allows the time it takes to reprime the arteries and rewet the circumferential wall grooves to be evaluated independently.

Arterial Deprime

An analysis of the arterial depriming characteristics has been previously presented by Peng and Peterson[6] for external artery configurations (see Fig. 2). This investigation resulted in a closed-form solution for the liquid column lengths in the liquid and vapor arteries with respect to time for the case of a constant longitudinal acceleration. Utilizing this technique, the correct energy balance for an arterial heat pipe can be expressed as

$$\rho_l a(H - x) - (2\sigma/R_l) + (2\sigma/R_v) = \tfrac{1}{2}\rho_l v_x^2 \qquad (1)$$

Arterial Reprime/Rewetting

Once the longitudinal acceleration is discontinued, the liquid column will begin to reprime the liquid artery in the same manner as that discussed in previous investigations.[4,5] Although accurately predicting the isothermal priming characteristics of external artery heat pipes, these analyses did not take into account the possibility of the fluid repriming a hot evaporator, and additionally, the possibility of an imposed heat flux present over the evaporator section. For a time $\tau = 0$, defined as the point at which the acceleration equals zero, the liquid channel column will advance toward the evaporator with a velocity U (see Fig. 3). This velocity is a function of time and of the corresponding liquid channel column length, thus, $U = U(\tau, H)$. A force-momentum balance on a control volume around the liquid column H can be written as

$$F_{cap} - F_{fricl} = \frac{d}{dt}(mU) \qquad (2)$$

or

$$2A_l\left(\frac{\sigma_l}{R_l} - \frac{\sigma_v}{R_v}\right) - \tau_w HP_l = \rho_l A_l\left(H\frac{dU}{d\tau} + U\frac{dH}{d\tau}\right) \qquad (3)$$

where the two terms on the left side of Eq. (3) represent the capillary forces acting on the two ends of the liquid control volume and the wall shear stress opposing the liquid column motion, respectively. The surface tension of the liquid column is allowed to vary with respect to the two ends, as the surface tension at the leading edge of the advancing liquid column will change after it has contacted a hot evaporator. The surface tension was evaluated, after contact with the evaporator, using the average temperature between the condenser and superheated evaporator. The two terms on the right side of Eq. (3) represent the change in momentum due to changes in velocity and changes in column mass, respectively. The differential time $d\tau$ may be found from the relationship

$$d\tau = \frac{dH_l}{U} \qquad (4)$$

and using a conservation of mass relationship, the differential rate of change of the liquid column dH_l and the differential rate of change of the liquid length dH is given by

$$dH_l = \frac{dH}{[1 + (A_l/A_v)]} = \frac{dH}{c_1} \qquad (5)$$

Assuming the liquid channel flow is laminar, the wall shear stress can be represented as

$$\tau_w = (8\mu_l U/D_l) \qquad (6)$$

Substituting Eqs. (4) and (6) into Eq. (3) and rearranging, yields an expression for the rate of change in the liquid column velocity with respect to the liquid column length, or

$$\frac{dU}{dH} = \frac{2}{c_1\rho_l HU}\left(\frac{\sigma_l}{R_l} - \frac{\sigma_v}{R_v}\right) - \frac{8\pi\mu_l}{c_1\rho_l A_l} - \frac{U}{H} \qquad (7)$$

where the appropriate boundary condition is $U = 0$ at $H = H_{initial}$ ($\tau = 0$). Equation (7) can be solved numerically to determine the liquid column velocity as a function of the liquid column length. The time required for the liquid column to advance to any specific point may be determined from the integration of Eq. (4), using the corresponding results from the solution to Eqs. (7) and (5).

For the case when the liquid column has advanced to the inlet of the evaporator, a portion of the advancing fluid is vaporized due to an evaporator wall superheat ΔT, and/or an imposed evaporator heat flux Q. The remaining fluid then advances at a velocity U_w, referred to as the rewetting velocity.

In the event that no wall superheat or evaporator heat flux is present, the rewetting velocity is simply equal to the velocity of the advancing liquid column, or U. The rewetting velocity can be determined with respect to the liquid column velocity by applying the conservation of energy to a control volume containing the portion of the liquid column located in the evaporator section at a specific instant in time (see Fig. 3), or

$$\dot{m}_v h_f = \rho_l A_l h_f (U - U_w) = h_f \dot{m}_{\text{grooves}} + c_p \Delta T A_c \rho_s \frac{dH_l}{d\tau} \quad (8)$$

where $\dot{m}_v$ is the vaporization rate of the liquid and is equal to the mass flow rate supplied to the wetted wall grooves plus the mass evaporated due to axial wetting of a portion of the superheated heat pipe evaporator section. The cross-sectional area A_c must include not only the cross-sectional area of the heat pipe, but the fin array as well, thus incorporating the entire thermal mass of the respective system.

Recognizing that once the liquid column has extended into the evaporator section, the differential change in the liquid column length with respect to time is equal to the rewetting velocity, or

$$U_w = \frac{dH_l}{d\tau} \quad (9)$$

For this case, the mass evaporated in the wetted grooves is equal to the total heat input to the evaporator multiplied by the ratio of the reprimed evaporator length to the overall evaporator length, or

$$\dot{m}_{\text{grooves}} = \frac{H_l - (L_c + L_t)}{L_e} \frac{Q}{h_f} \quad (10)$$

where L_e, L_c, and L_t are the lengths of the evaporator, condenser, and transport sections, respectively. Substituting Eqs. (9) and (10) into Eq. (8) and solving for the rewetting velocity yields the expression

$$U_w = \frac{\rho_l h_f A_l U - \left(\frac{H_l - (L_c + L_t)}{L_e}\right) Q}{\rho_l h_f A_l + c_p A_c \rho_s \Delta T} \quad (11)$$

where U is determined from the liquid column solution [Eqs. (4), (5) and (7)]. However, when liquid contacts the hot evaporator section, thereby initiating vaporization and fluid circulation due to the corresponding evaporation/condensation process, the pressure gradients (losses) due to the vapor mass flow rate and increased liquid mass flow rate must be included in the force-momentum relationship of Eq. (1). Since these pressure losses reduce the maximum capillary pumping pressure available, the rewetting velocity will be correspondingly reduced. These pressure losses are easily determined from the standard pressure gradient equations found in standard heat pipe analyses.

From Eq. (11), several characteristics are apparent:

1) In the case of no added heat input ($Q = 0$), and no wall superheat ($\Delta T = 0$), U_w is equal to U.

2) Increasing either the wall superheat or the heat input rate will decrease the rewetting velocity.

3) For the case of no heat addition, the liquid channel will reprime for any initial value of wall superheat, although at a decreasing rate for increasing superheat levels.

4) A heat input value of Q exists such that the rewetting velocity may become equal to zero, i.e., the liquid supply rate is equal to the vaporization rate and the advancing liquid column will stagnate.

Wall Groove Rewetting

The analysis of wall groove rewetting assumes that the wall grooves remain completely dry until the base (axial slot) of the groove is primed with liquid. As a result, each individual wall groove may be analyzed separately. Inherent in this method is the assumption of negligible axial conduction to the groove. This procedure has been presented by Peng et al.[7] Several basic assumptions in the analysis are normally made to simplify the expressions. These include laminar liquid flow in the groove, constant liquid properties, and the reduction of the characteristic groove dimensions to an effective capillary radius.

The primary difficulty in properly evaluating the rewetting velocity is effectively determining the net heat transfer rate to the liquid column. In the analysis of Peng et al.,[7] a uniformly applied heat flux along the circumference was assumed. However, for the specific case of rewetting the circumferential wall grooves in the two heat pipe configurations in this analysis, this assumption is no longer valid. The net heat transfer rate is assumed in this analysis to be one dimensional.

The assumption of negligible wall superheat for the specific case under investigation is based on examination of the measured temperature difference between the corresponding vapor and liquid channel temperatures at the same axial location. The dominate factor in decreasing the level of wall superheat at a specific axial position is the repriming of the liquid channel artery, as verified by the analysis of the SHARE II data. Once the liquid artery is filled to a specific point, the wall grooves rewet rapidly. However, it should be noted that with constant bus temperature boundary conditions occurring in the EATCS, this may or may not occur, since the net heat flux added to the advancing meniscus will be a direct function of the meniscus location, i.e., $f(\theta)$, the temperature difference between the heat pipe fluid and the bus vapor, the thermal resistances (including all bulk thermal resistances and any interfacial contact resistances) between the thermal bus and heat pipe fluids, and the overall thermal mass of the system.

Results

The transient temperature distributions and evaporator power levels for the LMSC/LTV Deprime II and III test cases and the NASA/GAC Deprime II test case are presented in Figs. 4–6 and correspond to the conditions given in Table 1. The two Deprime I and the NASA/GAC Deprime III results are not presented because no deprimings were observed for these cases. Presented in Figs. 4–6 are the measured vapor channel temperatures in the evaporator (E) section of the heat pipe, and a condenser (C) temperature measured on the radiating fin surface, directly above the heat pipe. The presented axial position x is measured from the evaporator end of the heat pipe. As seen from these three figures, the location of the

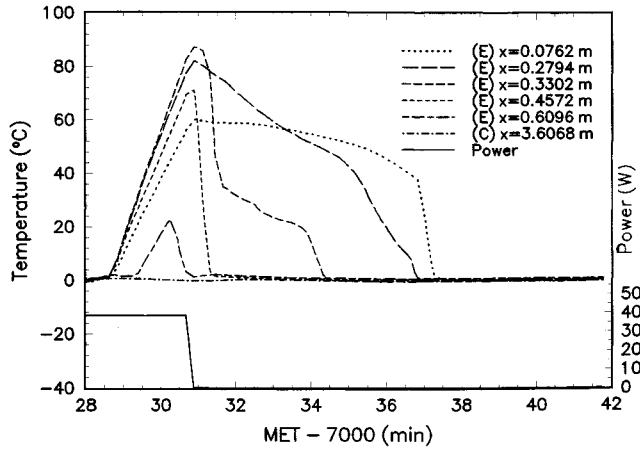

Fig. 4 NASA/GAC Deprime II temperature distribution.

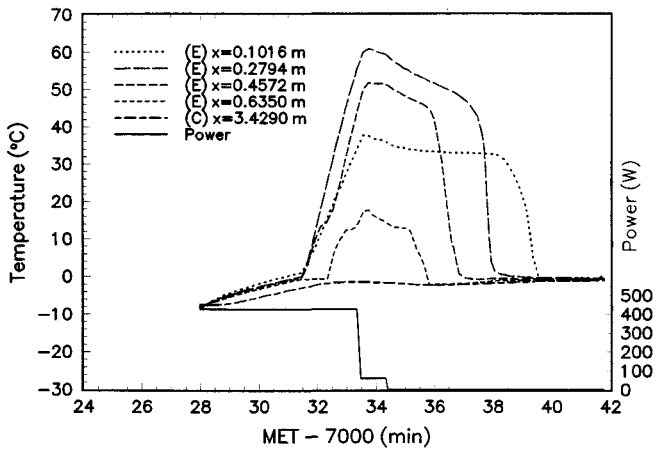

Fig. 5 LMSC/LTV Deprime II temperature distribution.

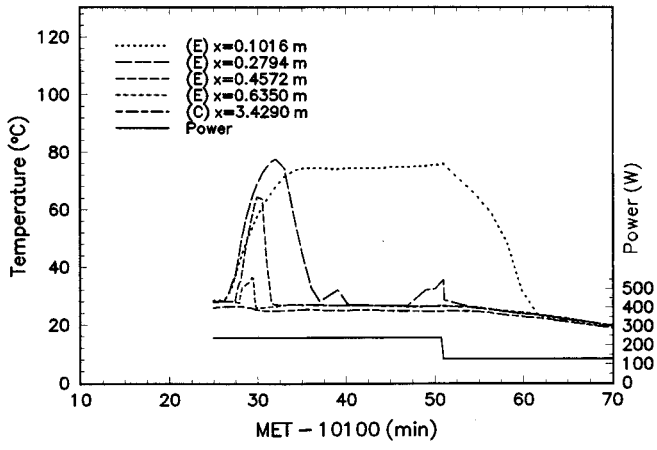

Fig. 6 LMSC/LTV Deprime III temperature distribution.

rewetting front is clearly defined for each case from the temperature measurements. However, the location of the liquid column during the acceleration induced depriming states cannot be accurately determined from the temperature measurements, thus, comparison of the analytical models with the flight test results is limited to the rewetting analyses.

Arterial Deprime

Examination of the resulting arterial deprime test results indicated that full evaporator depriming occurred for the LMSC/LTV heat pipe in both the Deprime II and III tests, while only in the Deprime II for the NASA/GAC. Although the LMSC/LTV test results were quite consistent, the two NASA/GAC tests demonstrated some inconsistencies due to variations in the initial condition for the two tests.

In the NASA/GAC Deprime II test, the evaporator was undergoing an evaporator dryout prior to initiation of the acceleration, thus the monogroove slot was deprimed prior to the acceleration. For the Deprime III test, the evaporator was fully primed, along with the connecting slot, and the heat pipe was operating properly. When the acceleration in the Deprime III test was applied, no communication of vapor between the vapor and liquid channels in the evaporator end would be available until the meniscus in the slot ruptured. The acceleration resulted in a "suction" on the receding liquid channel column and a "compression" effect on the advancing vapor channel column. This phenomena has been experimentally and analytically verified in previous heat pipe priming investigations.[4,5] The meniscus in the slot will only rupture when the pressure difference due to the compression-suction effect is greater than the capillary pressure capability of the slot or the axial hydrostatic height of the column in the slot exceeds the capillary pumping capability. However, no rupture in the slot occurred for this test case. The analysis examined in this investigation requires the vapor pressure to be equal in both channels.

In the previously developed closed-form solutions, only inertial and capillary forces were considered in the depriming analysis, thus neglecting the frictional losses in the receding liquid column. This assumption of negligible frictional forces, although valid for relatively shorter heat pipe lengths, will not be valid for the current configurations with overall lengths of 6.7 m. Therefore, frictional effects must be included to accurately determine the liquid column lengths.

Utilizing the same basic approach and assumptions as Peng and Peterson,[6] the liquid configuration at an arbitrary time τ, after the onset of the acceleration, is illustrated in Fig. 2, where H_l and H_v are the length of the liquid column in the liquid and vapor channels, respectively. Although when properly charged and primed, H_v would be zero at $\tau = 0$, some liquid may be located at the far end of the condenser region due to overcharging. In order to evaluate how the liquid configuration varies with time, a coordinate system was selected with its origin at the location of the liquid level in the vapor channel. At any position x' and time τ, an energy balance can be written to determine the velocity v_x of the liquid flowing from the liquid channel, through the axial slot, and into the vapor channel, and is expressed as

$$\int_{x'}^{H} \frac{dp}{dx'}\,dx' - \frac{2\sigma}{R_l} + \frac{2\sigma}{R_v} = \frac{1}{2}\rho_l v_x^2 \tag{12}$$

where the first term represents the frictional and gravitational head losses/gains, and the differential pressure drop dp/dx is given by

$$\frac{dp}{dx} = -\frac{(fRe)\mu\dot{m}(x)}{2A_l R_l^2 \rho} - \frac{2\dot{m}(x)}{A_l^2\rho}\frac{d\dot{m}(x)}{dx} + \rho a \tag{13}$$

Although the corresponding heat pipe depriming is a transient phenomena, the frictional pressure losses in the unsteady flow can be assumed to be approximately equal to steady flow frictional losses evaluated at the same instantaneous velocity, thus Eq. (13) is identical for flow occurring at steady state. This assumption has been shown to be accurate in numerous other experimental and theoretical investigations. The corresponding velocity distribution for the flow is found by solving Eq. (12) for v_x, and can be written as

$$v_x = \left[\frac{2}{\rho}\int_x^H \frac{dp}{dx}\,dx - \frac{4\sigma}{\rho_l}\left(\frac{1}{R_l} - \frac{1}{R_v}\right)\right]^{1/2} \tag{14}$$

As seen from Eq. (14), if the pressure gradient due to the acceleration load is less than the capillary pumping capability of the heat pipe, Eq. (14) results in a complex, and thus unrealistic, value. For this case, depriming will not occur for the given conditions. A position exists, H', such that when $x \geq H'$, the velocity v_x is equal to 0. The volumetric flow rate of liquid leaving the liquid channel at any time τ is determined by integrating the resulting velocity distribution multiplied by the width of the axial slot connecting the liquid and vapor channels δ over the length of the flow area, or

$$\dot{V}(\tau) = \int_0^{H'} \delta v_x\,dx \tag{15}$$

The corresponding change in volume of the liquid in the liquid channel is determined by

$$A_l\,dH_l = \dot{V}(\tau)\,d\tau \tag{16}$$

and from conservation of mass, the relationship between the differential changes in the liquid channel and vapor channel liquid heights is expressed as

$$A_l\,dH_l = -A_v\,dH_v \tag{17}$$

Using these relationships, the location of the liquid/vapor interface in the liquid channel and vapor channel can be determined for an acceleration applied over a specified time interval. Because the axial mass flow rate and the mass flow rate through the slot are directly related, a closed-form solution is not obtainable due to the inclusion of the axial mass flow rate in the frictional pressure drop terms. Thus, an iterative numerical solution must be employed for each time-step.

Arterial Reprime/Rewetting

Accurate determination of the time for the liquid channel to fully reprime requires the initial location of the fluid be known at the time when the acceleration is discontinued. Unfortunately, since this initial location is not available from the flight temperature profiles, an initial assumption for the initial liquid column heights must be made prior to analysis. For both heat pipes, the initial assumption that the liquid column height and the vapor column height were the same, thus $H = 0$, was selected. This assumption will be more accurate for the LMSC/LTV heat pipe than for the NASA/GAC heat pipe, due to the wider slot of the graded groove configuration causing increased sensitivity to depriming for a specific acceleration level.

The comparison of the analytical model with the data for the LMSC/LTV Deprime II and III tests, and the NASA/GAC Deprime II test are analyzed separately for each specific test. For all comparisons, a reference time of 0.0 s is used and defined as the point when the longitudinal acceleration is discontinued. In the LMSC/LTV Deprime II test, the parameters used in the analytical model consisted of assuming a constant evaporator superheat of 50°C, a heat input of 0 W, and fluid properties evaluated at the condenser temperature of −6°C. The value of superheat was chosen to represent an average value found in the experimental data. The theoretical liquid front position x (measured from the evaporator end of the heat pipe), is presented in Fig. 7, along with the experimental rewetting data obtained from the SHARE II temperature profiles. Rewetting by the liquid column was specified to be completed when the wall temperature was within 10°C of the condenser fluid temperature. Also presented in Fig. 7 for comparison is the liquid front position for an isothermal heat pipe without heat addition.

Examination of the theoretical liquid front position in Fig. 7 allows two physical points along the liquid artery of the heat pipe to be visible. The first is the point where the liquid column initiates contact with the liquid channel splitter. As the splitter decreases the capillary radius (thus increasing the capillary pumping pressure), the repriming front is accelerated and results in a more rapid rate of repriming. The second point is the inlet of the evaporator. For both values of evaporator wall superheat (0 and 50°C), the liquid front position is identical until it contacts the evaporator. The corresponding vaporization of a portion of the advancing meniscus for the wall superheat case, reduces the rate at which the liquid front advances, thereby clearly defining the inlet of the evaporator in Fig. 7.

From Fig. 7, the theoretical liquid position and the experimental data are not well correlated. Therefore, a new reference value of 0.0 s was defined as the point when the experimental rewetting front contacts the nearest thermocouple to the evaporator exit. The analytical solution was also referenced to this same point and time and the corresponding comparison is given in Fig. 8. For this case, the model slightly underpredicts the rewetting characteristics of the evaporator section, but exhibits the same fundamental trends as the experimental data. This underprediction may be due to the inherent difficulty of accurately determining the evaporator section thermal mass at a specific cross section and/or the assumption of a 50°C superheat, resulting in additional energy storage in fins and heater elements due to higher thermal mass or higher temperatures not accounted for in the analysis.

The LMSC/LTV Deprime III and NASA/GAC Deprime II tests are presented in Figs. 9 and 10, and Figs. 11 and 12, respectively, and use the same analysis procedure described for the above LMSC/LTV Deprime II case. The comparison of the LMSC/LTV Deprime III data and the analytical model in Fig. 10 are in good agreement for a wall superheat of 70°C and a heat input of 237 W. This increased theory/data agreement in Fig. 10 additionally supports the hypothesis that the thermal mass was underestimated in the LMSC/LTV Deprime II comparison. This is due to the increased influence of the 237-W heat input on the advancing liquid column position, and corresponding decreased influence of the wall superheat.

For the NASA/GAC Deprime II test presented in Fig. 12, the theoretical liquid front position significantly underpredicts the actual test data. This may be in part due to the underestimation of the thermal mass, but more likely results from the flow characteristics around the concentric screen inserts in the liquid channel artery. The only attempt to incorporate

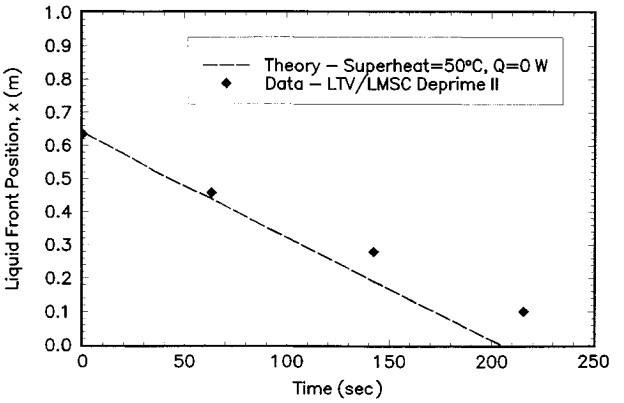

Fig. 8 Comparison of arterial reprime/rewetting analysis with LMSC/LTV Deprime II—evaporator only.

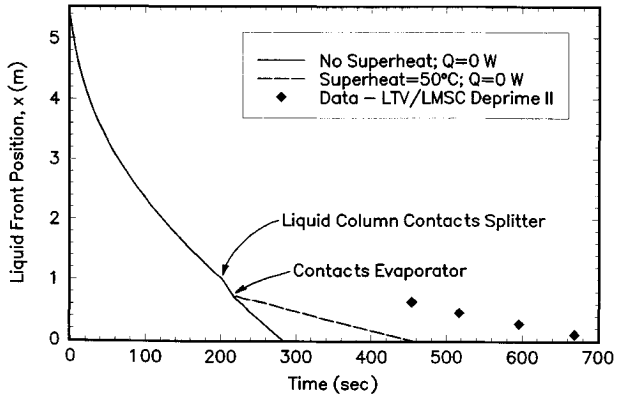

Fig. 7 Comparison of arterial reprime/rewetting analysis with LMSC/LTV Deprime II.

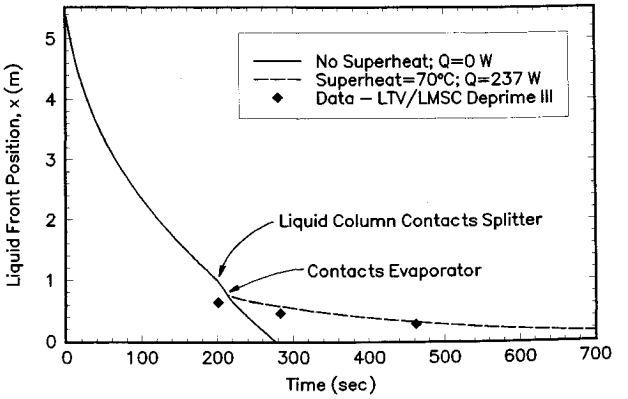

Fig. 9 Comparison of arterial reprime/rewetting analysis with LMSC/LTV Deprime III.

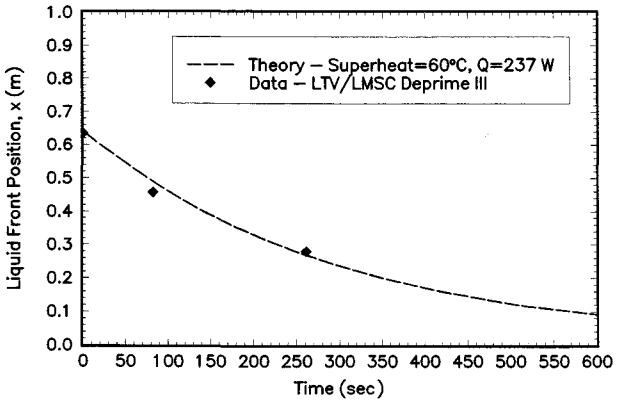

Fig. 10 Comparison of arterial reprime/rewetting analysis with LMSC/LTV Deprime III—evaporator only.

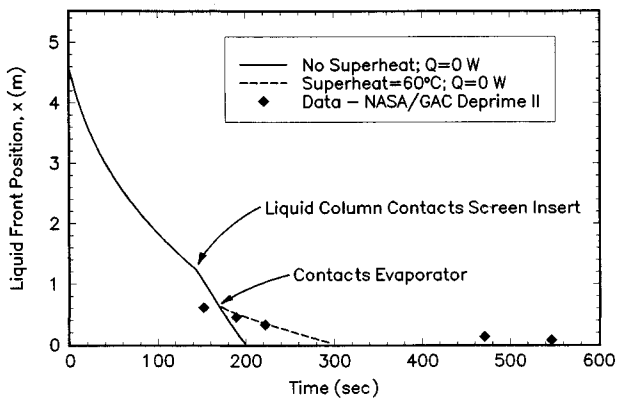

Fig. 11 Comparison of arterial reprime/rewetting analysis with NASA/GAC Deprime II.

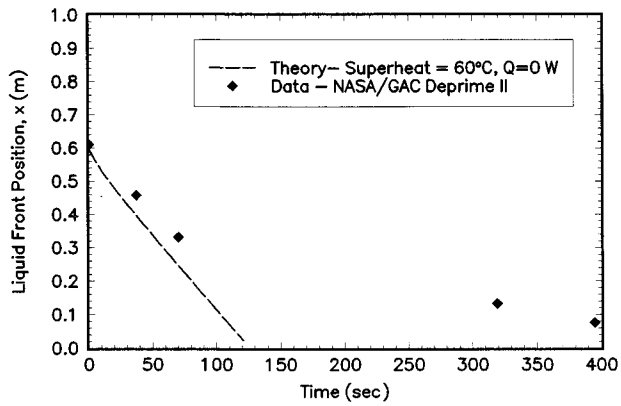

Fig. 12 Comparison of arterial reprime/rewetting analysis with NASA/GAC Deprime II—evaporator only.

these inserts into the analytical model was by accounting for the increased capillary pumping when the liquid column contacts the insert. However, added frictional pressure losses through the screen inserts and the characteristics of the more complicated flowfields in the screen inserts (i.e., the liquid filling of the inner annulus prior to the actual channel) were not included and are the likely source for the model/data discrepancy.

As discussed in the development of the arterial reprime/rewetting analysis, one important factor should be again noted. This relates to the maximum capillary pressure available to pump the advancing liquid artery column. When the liquid column extends into the evaporator section, the vaporization/condensation process results in vapor channel frictional losses and increased liquid channel losses. These added losses decrease the overall available pumping pressure for driving the rewetting front. While not as severe in the wall superheat case, these losses may become great enough in the case of an applied heat flux (including evaporator coupling to a constant temperature thermal bus) that the rewetting velocity will become zero. When the rewetting velocity becomes zero, the heat pipe operation corresponds to the heat pipe capillary limit, with the maximum capillary pressure based on the liquid channel capillary radius and not the axial groove radius. As shown in Fig. 6, this case of a stagnant rewetting front occurred for the LMSC/LTV Deprime III test. Final rewetting of the evaporator did not occur until the heat input was reduced.

Wall Groove Rewetting

Once liquid contact occurs at the base of a specific wall groove, rewetting is anticipated to be quite rapid, due to the small capillary radius of the groove and the excellent wetting characteristics of ammonia. To verify that the rewetting time for low heat input levels and no wall superheat is rapid, a typical wall groove with an effective capillary radius of 0.031 mm was analyzed using the method of Peng et al.[7]—with the fluid properties evaluated at a temperature of 20°C. The time required to fully reprime an individual groove was found to be approximately 0.13 s. Additionally, the effects of a 385-W heat input over the entire evaporator length was examined and shown to have negligible effects on the rewetting front. It is important to note that this negligible effect at 385 W does not imply an overall insensitivity in the rewetting velocity to heat transfer, but instead demonstrates the negligible effects at low loads.

Conclusions

An overall analysis of the depriming and repriming/rewetting characteristics for high-capacity external artery heat pipes was conducted. This investigation utilized recent microgravity flight data from two different heat pipe configurations, an existing acceleration induced depriming analysis, an existing circumferential wall groove rewetting analysis, and an arterial reprime/rewetting analysis. Combining these three processes, a technique was developed by which the effect of external accelerations on the operational characteristics of these two heat pipes could be predicted.

The only existing arterial depriming model did not include frictional losses and, thus, a comparison with the NASA/GAC and LMSC/LTV heat pipes in acceleration environments was not possible. While frictional effects may be neglected for relatively short heat pipes, these losses must be included for the long (6.7-m) heat pipes proposed for use on Space Station Freedom. The present arterial reprime/rewetting analysis and a previous wall groove rewetting analysis were both found to agree favorably with the reprime/rewetting data obtained from the SHARE II flight experiment deprime tests of two high-capacity external artery heat pipes. Examination of arterial reprime/rewetting and wall groove rewetting characteristics revealed that the time required for complete recovery of a deprimed evaporator is dominated by the liquid artery rewetting. Since the wall grooves will prime only after liquid has contacted the axial slot, the overall evaporator recovery time is not significantly affected by the wall groove rewetting time for low heat input loads.

Acknowledgment

The authors would like to acknowledge the support by NASA/JSC under NASA Grant NAG9-511.

References

[1]Raetz, J., and Domonick, J., "Space Station External Thermal Control System Design and Operational Overview," Society of Automotive Engineers, SAE Paper 921106, July 1992.

[2]Brown, R., Kosson, R., and Ungar, E. K., "Design of the SHARE II Monogroove Heat Pipe," AIAA Paper 91-1359, June 1991.

[3]Ambrose, J., and Holmes, H. R., "Development of the Graded Groove High Performance Heat Pipe," AIAA Paper 91-0366, Jan. 1991.

[4]Peterson, G. P., and Marshall, P. F., "Experimental and Analytical Determination of Heat Pipe Priming in Micro-G," *Research and Development in Heat Pipe Technology*, edited by K. Oshima, Vol. 1, JaTec Publishing Co., Tokyo, Japan, 1984, pp. 434–439.

[5]Peterson, G. P., and Annamalai, N. K., "A Differential Approach to Heat Pipe Priming in Microgravity," *Chemical Engineering Communications*, Vol. 52, Nos. 1–3, 1987, pp. 151–167.

[6]Peng, X. F., and Peterson, G. P., "Acceleration Induced Depriming of External Artery Heat Pipes," *Journal of Thermophysics and Heat Transfer*, Vol. 6, No. 3, 1992, pp. 546–548.

[7]Peng, X. F., Peterson, G. P., and Lu, X. J., "Analysis of Capillary Induced Rewetting in Circular Channels with Internal Grooves," *Journal of Thermophysics and Heat Transfer*, Vol. 7, No. 2, 1993, pp. 334–339.

[8]Kosson, R., Brown, R., and Ungar, E. K., "Space Station Heat Pipe Advanced Radiator Element (SHARE) Flight Test Results and Analysis," AIAA Paper 90-0059, Jan. 1990.

[9]Brown, R., Ungar, E. K., and Cornwell, J. D., "Flight Test Results of the SHARE II Monogroove Heat Pipe," AIAA Paper 92-2886, July 1992.

[10]Ambrose, J., Holmes, H. R., Cima, R. M., and Kapolnek, M. R., "Flight Test Results for a High Capacity Single Groove Heat Pipe," AIAA Paper 92-2887, July 1992.